Eur. Phys. J. C 50, 53–62 (2007)
DOI 10.1140/epjc/s10052-006-0205-3

THE EUROPEAN PHYSICAL JOURNAL C

Regular Article – Theoretical Physics

Next-to-leading logarithms and the PHOTOS Monte Carlo

P. Golonka[1,a], Z. Wąs[2]

[1] CERN, 1211 Geneva 23, Switzerland
[2] Institute of Nuclear Physics, PAN, Kraków, ul. Radzikowskiego 152, Poland

Received: 11 August 2006 / Revised version: 17 November 2006 /
Published online: 3 February 2007 –

Abstract. The PHOTOS Monte Carlo program is often used for the simulation of experimental, selection-sensitive, QED radiative corrections in decays of Z bosons and other heavy resonances and particles. The present paper will be devoted to those parts of the next-to-leading order corrections for leptonic Z decays which are normally missing in PHOTOS. The analytical form of the exact and truncated, *standard*, kernel used in PHOTOS will be explicitly given. The correction, being the ratio of the exact to the approximate kernel, can be activated as an optional contribution to the internal weight of PHOTOS. We will quantify the numerical effect of the approximation with the help of a multitude of distributions. The numerical size of the effect is in general below 0.1%; however, in some corners of the phase space (well defined and contributing less than 0.5% to the total rate), it may reach up to about 20% of their relative size.

1 Introduction

With the approaching start-up of the experiments at LHC, the urgency to quantify systematic uncertainties of the generators, used in the interpretation of the data, is becoming pressing.

A well-defined class of theoretical effects consists of the QED radiative corrections. PHOTOS is a universal Monte Carlo algorithm that simulates the effects of these corrections in decays of particles and resonances. It is a project with a rather long history: the first version was released in 1991 [1], followed by version 2.0 [2] (double emission, threshold terms for fermions). The package is in wide use [3]: it was applied as a precision simulation tool for W mass measurement at the Tevatron [4] and LEP [5, 6], and for CKM matrix measurements in decays of K and B resonances (NA48 [7], KTeV [8], Belle [9], BaBar [10] and at Fermilab [11]).

Throughout the years the core algorithm for the generation of $O(\alpha)$ corrections did not change much; however, its precision, applicability to various processes, and numerical stability improved significantly. New features, such as multiple-photon radiation or interference effects for all possible decays, were also introduced.

Growing interest in the algorithm expressed by the experimental collaborations (including the future LHC experiments) and its applications in analysis of the measured experimental data was a motivation to perform a more detailed study of the potential and precision of the PHOTOS algorithm.

The present paper is the third in a series [12, 13]. It is devoted to the Z boson decay (namely the $e^+e^- \to Z^0/\gamma^* \to \mu^+\mu^-(\gamma)$ process), and to simplifications in the matrix element used in PHOTOS for that channel. Thanks to complete phase-space coverage in the program, it is possible to implement with no approximations the exact matrix element for any decay channel. To calculate the complete matrix element for, say, the Z decay, however, additional information such as the effective Born-level Z/γ^* couplings or beam directions need to be provided. Its implementation would have made the PHOTOS solution less modular and thus less convenient for the users. That is why we choose to explore numerically the limitations originating from the compromises introduced into the PHOTOS bremsstrahlung kernel and remain with a solution which assures convenience of use; process-dependent weight may still be avoided.

The paper is organized as follows. In Sect. 2 the main properties used in the PHOTOS design and, in particular, the analytical form of the (NLO) weight, necessary to introduce the complete first-order matrix element, are presented. In Sect. 3, those aspects of the program construction which are relevant to the use of the NLO weight with multiple-photon generation are briefly presented. In Sect. 4 the method used for numerical comparisons is explained. Section 5 presents the results of numerical tests of PHOTOS, performed at fixed first order of the QED expansion. Since the program uses the same building block for a part of the single-photon generation algorithm and for the multiple bremsstrahlung, the results presented in this section provide a technical test of the main building block of multi-photon radiation in PHOTOS. These results are compared later with the ones of the tests for multiple-

[a] e-mail: Piotr.Golonka@CERN.CH

photon simulation of PHOTOS, collected in Sect. 6. A summary, Sect. 7, closes the paper.

Section 2 explains also how the inclusion of complete matrix elements breaks the separation of the final-state bremsstrahlung effects from the Born-level scattering description, making the algorithm less flexible.

Finally, some readers may find in Sect. 2 the material for a discussion of the PHOTOS matrix element and of the Monte Carlo phase-space algorithm, possibly stimulating understanding of the practical solutions of the improved expansions for description of multi-body final states. Some aspects of our solution resemble those of classical exclusive exponentiation as described in [14, 15]; in the others, similarities to the parton shower may be identified. It may be understood as a rearrangement of the QED perturbation expansion; yet this point will not be discussed here. Instead, let us point out some similarities of the PHOTOS solution to the methods discussed elsewhere: the interaction picture of quantum mechanics, expansion of special functions around asymptotic solutions [16] or in field theory [17]. In PHOTOS the expansion is performed in terms of multidimensional operators. The detailed phase-space parametrization (which can be found in [28]) is essential to understand the details. A multitude of footnotes is devoted to that less focused topic of our paper.

2 Phase space and matrix element

To discuss the implementation of the complete first-order QED radiative corrections in Z decay, we need detailed parametrization of the phase space. In the early papers on PHOTOS [1, 2] the question of the phase-space parametrization was not covered in sufficient detail and, in particular, the correctness and completeness of the multi-body phase space implemented in the program was not emphasized. Recently, this point has been discussed in detail in [28]: various parts of PHOTOS Monte Carlo weights responsible for phase space are given explicitly there. We would like to stress that the phase-space-related weights are fully separated from the ones for the matrix element (the latter containing different types of approximations). All terms depending on masses of final-state particles are explicitly given in the phase-space parametrization; this essential part of the algorithm description will, however, not be described here.

Let us write the explicit form of the real-photon matrix element (for the first time separated from the phase-space Jacobians), as used in the standard version of PHOTOS (as published in [1, 2]) for the $e^+e^- \to Z^0/\gamma^* \to \mu^+\mu^-(\gamma)$ process:

$$
\begin{aligned}
&X_f^{\mathrm{PHOTOS}} \\
&= \frac{Q'^2\alpha(1-\Delta)}{4\pi^2 s} s^2 \Bigg\{ \frac{1}{k'_+ + k'_-}\frac{1}{k'_-} \\
&\times (1+(1-x_k)^2)\frac{\mathrm{d}\sigma_B}{\mathrm{d}\Omega}\left(s, \frac{s(1-\cos\Theta_+)}{2}, \frac{s(1+\cos\Theta_+)}{2}\right) \\
&\times \frac{(1+\beta\cos\Theta_\gamma)}{2} \\
&+ \frac{1}{k'_+ + k'_-}\frac{1}{k'_+} \\
&\times (1+(1-x_k)^2)\frac{\mathrm{d}\sigma_B}{\mathrm{d}\Omega}\left(s, \frac{s(1-\cos\Theta_-)}{2}, \frac{s(1+\cos\Theta_-)}{2}\right) \\
&\times \frac{(1-\beta\cos\Theta_\gamma)}{2} \Bigg\}, \qquad (1)
\end{aligned}
$$

where $\Theta_+ = \angle(p_+, q_+)$, $\Theta_- = \angle(p_-, q_-)$; $\Theta_\gamma = \angle(\gamma, \mu^-)$ is defined in the (μ^+, μ^-) pair rest frame. It is to be compared with the exact expression, taken from [21]:

$$
\begin{aligned}
X_f &= \frac{Q'^2\alpha(1-\Delta)}{4\pi^2 s} s^2 \\
&\times \Bigg\{ \frac{1}{(k'_+ + k'_-)}\frac{1}{k'_-}\left[\frac{\mathrm{d}\sigma_B}{\mathrm{d}\Omega}(s,t,u') + \frac{\mathrm{d}\sigma_B}{\mathrm{d}\Omega}(s,t',u)\right] \\
&+ \frac{1}{(k'_+ + k'_-)}\frac{1}{k'_+}\left[\frac{\mathrm{d}\sigma_B}{\mathrm{d}\Omega}(s,t,u') + \frac{\mathrm{d}\sigma_B}{\mathrm{d}\Omega}(s,t',u)\right] \Bigg\}. \qquad (2)
\end{aligned}
$$

In the presented formulae we follow the notation from [21] (where the interested reader may find details of the definitions of all variables and expressions), in particular:

$$
\begin{aligned}
s &= 2p_+\cdot p_-\,, \quad & s' &= 2q_+\cdot q_-\,, \\
t &= 2p_+\cdot q_+\,, \quad & t' &= 2p_+\cdot q_-\,, \\
u &= 2p_+\cdot q_-\,, \quad & u' &= 2_-\cdot q_+\,, \\
k'_\pm &= q_\pm\cdot k\,, \quad & x_k &= 2E_\gamma/\sqrt{s}\,. \qquad (3)
\end{aligned}
$$

The Δ term encapsulates final-state mass-dependent terms; p_+, p_-, q_+, q_-, k denote four-momenta of incoming e^+, e^-, outgoing μ^+, μ^- and the bremsstrahlung photon respectively.

The ratio of (2) to (1) constitutes the upgrade of PHOTOS to the complete first order.[1] Nothing needs to be changed in the phase-space parametrization; yet the effects of the virtual corrections have to be included in the normalization. The combined effect of the virtual and real corrections on the total rate is an increase by a factor of $1+\frac{3}{4}\frac{\alpha}{\pi}$. The expression for the correcting weight could be defined[2] as

$$
\mathrm{WT} = \frac{X_f}{X_f^{\mathrm{PHOTOS}}}\frac{1}{\left(1+\frac{3}{4}\frac{\alpha}{\pi}\right)}. \qquad (4)
$$

For the purpose of constructing a Monte Carlo algorithm, however, it is more convenient to separate the generation into a sum of two branches (with slightly different angular variable mapping). The expression, properly normalized

[1] This is only true for PHOTOS being run at first order. For the multiple-photon radiation option, the iteration of the single-photon emission kernel (and thus also its weight) is performed; see Sect. 5.

[2] Alternatively, a factor $(1+\frac{3}{4}\frac{\alpha}{\pi})$ can be included in the definition of the crude distribution.

for virtual corrections, reads

$$
\begin{aligned}
X_f &= X_f^1 + X_f^2 .\\
X_f^1 &= \frac{\mathrm{d}\sigma_B}{\mathrm{d}\Omega}\left(s, \frac{s(1-\cos\Theta_+)}{2}, \frac{s(1+\cos\Theta_+)}{2}\right)\\
&\quad \times X_f^{\mathrm{PHOTOS1}} \mathrm{WT}_1 ,\\
X_f^2 &= \frac{\mathrm{d}\sigma_B}{\mathrm{d}\Omega}\left(s, \frac{s(1-\cos\Theta_-)}{2}, \frac{s(1+\cos\Theta_-)}{2}\right)\\
&\quad \times X_f^{\mathrm{PHOTOS2}} \mathrm{WT}_2 .
\end{aligned} \tag{5}
$$

Instead of a single weight (4), two weights WT_1 and WT_2 for the respective two branches of the generation appear:

$$
\begin{aligned}
&\mathrm{WT}_1 = \\
&\left(\frac{\mathrm{d}\sigma_B}{\mathrm{d}\Omega}(s,t,u') + \frac{\mathrm{d}\sigma_B}{\mathrm{d}\Omega}(s,t',u)\right) \Bigg/ \\
&\left\{\left[\left(1+(1-x_k)^2\right)\frac{\mathrm{d}\sigma_B}{\mathrm{d}\Omega}\left(s, \frac{s(1-\cos\Theta_+)}{2}, \frac{s(1+\cos\Theta_+)}{2}\right)\right]\right.\\
&\left.\times \frac{(1+\beta\cos\Theta_\gamma)}{2}\left(1+\frac{3}{4}\frac{\alpha}{\pi}\right)\right\} ,\\
&\mathrm{WT}_2 = \\
&\left(\frac{\mathrm{d}\sigma_B}{\mathrm{d}\Omega}(s,t,u') + \frac{\mathrm{d}\sigma_B}{\mathrm{d}\Omega}(s,t',u)\right) \Bigg/ \\
&\left\{\left[\left(1+(1-x_k)^2\right)\frac{\mathrm{d}\sigma_B}{\mathrm{d}\Omega}\left(s, \frac{s(1-\cos\Theta_-)}{2}, \frac{s(1+\cos\Theta_-)}{2}\right)\right]\right.\\
&\left.\times \frac{(1-\beta\cos\Theta_\gamma)}{2}\left(1+\frac{3}{4}\frac{\alpha}{\pi}\right)\right\} .
\end{aligned} \tag{6}
$$

At this point let us make some remarks that may be of interest only if one aims at future extensions of the presented analysis. Even though the introduction of the NLO weight into PHOTOS is trivial, the approximation developed [1] at the heart of the PHOTOS design is not. It enabled universality of the program.[3] Simplification was not necessary to attribute the generation of bremsstrahlung photons to individual charged particles.[4] The separation holds for the complete NLO as well.

The simplified emission kernels $X_f^{\mathrm{PHOTOS}\,1,2}$, which we use for simulation of bremsstrahlung in PHOTOS for all other decays as well, can be easily identified in (1); let us write them explicitly now:

$$
\begin{aligned}
&X_f^{\mathrm{PHOTOS}} = \\
&\frac{\mathrm{d}\sigma_B}{\mathrm{d}\Omega}\left(s, \frac{s(1-\cos\Theta_+)}{2}, \frac{s(1+\cos\Theta_+)}{2}\right) X_f^{\mathrm{PHOTOS1}}\\
&+ \frac{\mathrm{d}\sigma_B}{\mathrm{d}\Omega}\left(s, \frac{s(1-\cos\Theta_-)}{2}, \frac{s(1+\cos\Theta_-)}{2}\right) X_f^{\mathrm{PHOTOS2}} ,\\
&X_f^{\mathrm{PHOTOS1}} = \\
&\frac{Q'^2\alpha(1-\Delta)}{4\pi^2 s} s^2 \frac{1}{k'_+ + k'_-}\frac{1}{k'_-}\left(1+(1-x_k)^2\right)\frac{(1+\beta\cos\Theta_\gamma)}{2} ,\\
&X_f^{\mathrm{PHOTOS2}} = \\
&\frac{Q'^2\alpha(1-\Delta)}{4\pi^2 s} s^2 \frac{1}{k'_+ + k'_-}\frac{1}{k'_+}\left(1+(1-x_k)^2\right)\frac{(1-\beta\cos\Theta_\gamma)}{2} .
\end{aligned} \tag{7}
$$

These emission kernels depend on the spin and charge of the "emitting particle" only and do not depend on the properties of the other decay products. Other decay products define the phase-space limits only.[5] To obtain the universal form of the photon emission kernel, the interference term was eliminated with the help of the factor, either $\frac{2}{(1+\beta\cos\Theta_\gamma)}$ or $\frac{2}{(1-\beta\cos\Theta_\gamma)}$. The interference was recovered later, using the weight given in formula (17) of [2]; that is, with an approximation. On the other hand, having paid the price of the approximated solution, both the kernel and the interference weight could be used for the decay of any particle or resonance.

In the present study the process $e^+e^- \to Z^0/\gamma^* \to \mu^+\mu^-$ is discussed; both the approximate weight of [2] and our formula (6) will be used. In principle, a similar study can be performed for any other decay, if only a matrix element is available. For decays such as $B^0 \to \pi^+K^-$ an analysis was already completed [28].

3 Algorithm for multiple-photon generation

The question of the use of the complete first-order matrix element for the kinematical configurations, where more than one hard photon is present, requires individual study and verification. Such a discussion remains out of the scope of the present paper. Nonetheless, let us comment on those technical details of the PHOTOS algorithm that are important in the implementation of the NLO contribution to the correcting weight.

[3] Indeed, after inspection, the differences between formulae (1) and (2) are quite significant. The exact expression does not allow one to transfer the complete Born-level angular dependence to the host generator. In the correction weight, the two contributions, one depending on the angle Θ_+ and another on Θ_-, have to be simultaneously included. The dependence on the Born-level (effective) couplings thus need to be known when calculating the final-state bremsstrahlung weight. This would make the modular structure of PHOTOS more difficult to keep. Also, the direction of the (effective) beam would need to be provided to calculate the Θ_+ and Θ_- angles. This exhibits another difficulty in the separation of the final-state bremsstrahlung and the dynamics of Z/γ^* production.

[4] For other decays, it will probably not be necessary to find an explicit form of such NLO separation. Starting from the NNLO, such a separation was shown to be impossible [22] anyway.

[5] In the original PHOTOS documentation we called this well-controlled truncation of the kernel a "property (such) that leading-log (collinear) and infrared limits are properly reproduced". This explanation turned out to be misleading for many readers. One can get biased and expect the collinear approximation not only for the kernel, but for the whole design of the algorithm. This would be a serious limitation of our program design if indeed, as suggested in [23], "PHOTOS was based on a collinear approximation". Fortunately this is not the case. Such a confusion was not a concern for the users, until now: precision requirements were not as high.

The iteration algorithm, as explained first in [2], and recently also in [12,13], did not require changes at all. However, some details of the implementation of the NLO weight (formula (6)) need to be clarified. All identical terms present in the numerator and denominator, expressions (2) and (1), were cancelled analytically.[6] The weight (6) has to be calculated for the single-photon configuration. If there are other photons generated in the previous steps of the iteration, their momenta are absorbed into the momenta of the final-state fermions, as explained already in [2].

4 Method used in numerical tests

The definition of the validation strategy for the Monte Carlo tool aiming at representing results of field theory calculations, such as PHOTOS, represent a project in itself. Several aspects need to be covered. Also, the requirements of, say, experimental physicists analyzing precision data will differ from those interested in the backgrounds for rare process, or theorists interested in future extensions of the methods applied in PHOTOS.

As we aim to show how the implementation of exact first-order matrix element changes the prediction of PHOTOS simulations, we chose the distributions which can be used, and compared, not only in the case of simulations for single-photon emission, but also for multiple-photon simulations. The method has to be insensitive to the way how the soft singularities are regulated in PHOTOS and other programs used for the tests.

In our paper we will use the same method, based on MC-TESTER [24], as in [13] to work for QED bremsstrahlung in Z/γ^* leptonic decay. For convenience of the readers, let us recall a brief definition of that method.

For selected decay processes, such as Z/γ^* leptonic decays, the four-momenta of the decay products and their flavours are extracted (by MC-TESTER) from the event record in an automated way. The decay events obtained that way are classified in distinct decay channels, according to the particles present in the final state. The histograms of all possible invariant masses, which can be formed from the decay products, are defined and filled for each identified decay channel. At the end of the run they are stored in output files.

For each decay channel the plots of the histogrammed values are then produced; each plot presents two distributions, from the two distinctive runs, and a curve, which is the ratio of the two normalized distributions. The shape difference parameter[7] is calculated to quantify the difference between the two simulations for the same process by a single number.

If the results of different programs were compared blindly, ambiguities due to differences in the treatment of the soft-emission region and of the different boundaries for the photon phase space (integrated analytically) would arise. To prevent these ambiguities, the most convenient solution was to introduce a technical regulator *in the test itself*.

For our comparisons to make physical sense and remain automatic, we had to remove the softest photons from the final states. We defined zero-, one-, and two-photon topologies in the following way: we called the event "zero photon" if there was no photon of energy (in a decaying particle's rest frame) larger than $E_{\rm test} = 1\,\mathrm{GeV}$. The "one-photon" event had to have one (and only one) photon of energy larger than $E_{\rm test}$. If there were more than one such photon, we called it a "two-photon" event. In the case where there were more than two photons of energy larger than $E_{\rm test}$, we considered only the two most energetic ones, and treated the remaining (softer) ones as if they had not passed the $E_{\rm test}$ threshold. For all the photons that did not pass the $E_{\rm test}$ threshold we summed their four-momenta with the momentum of the outgoing fermion of smaller angular separation. With the help of this procedure we divide the phase space for two fermions and an arbitrary number of photons into *slots* of 0, 1 and 2 distinguished final-state photons.

In the paper we will use two variants of this test definition: *test1* and *test2*. The *test2* is exactly as explained above. In *test1*, only one photon (the most energetic one) will be accepted. The free parameter, $E_{\rm test}$ is chosen to be 1 GeV for all results presented in this paper.

Due to space limitations we will limit the presentation of the results to branching fractions of final states differing by the number of hard photons and SDP. Only two plots of largest SDP per comparison will be shown. For the complete set of comparison booklets we address the reader to the preprint version of our paper or to the web page [29].

With respect to our previous publications, we decided to modify the way in which the distributions are presented: a logarithmic instead of linear scale is used in all plots. This is to some degree against our choice of the SDP definition used here. For some readers, however, this may look more convenient, especially for cases of sharply peaked distributions. In the literature, to compare results from two distinct Monte Carlo programs it is quite common to present

[6] The cancelled terms could have been calculated using slightly different kinematical variables; the differences would have appeared only in the case of more than one hard photon present in the final state. In such a case the ratio of the terms would not be equal to 1. These effects generally go beyond the NLO, and in fact our choice was motivated by the comparisons with the second-order matrix-element calculation, but without necessary details. That is why an appropriate discussion of this choice would require a detailed presentation of the second-order matrix element. It would have to be similar, for example, to the discussion of the extrapolation procedure as that described in [26] for initial-state radiation in $e^+e^- \to \nu_e\bar{\nu}_e$ production.

[7] The shape difference parameter (SDP), defined in [24], quantifies the difference in shape of the histograms coming from the two runs being compared. The SDP value is calculated separately for each histogrammed mass: it quantifies the exclusive surface between the corresponding histograms (normalized to unity) obtained from the two runs. The effects of statistical fluctuations are appropriately subtracted. The maximum SDP over all distributions for a given decay channel is taken and printed in a summary table.

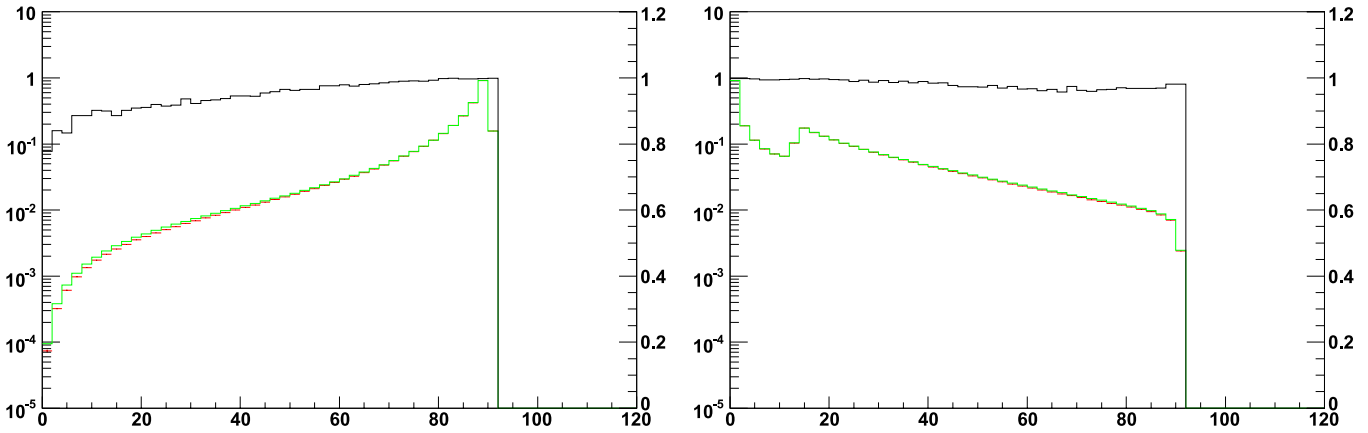

Fig. 1. Comparison of standard PHOTOS and KORALZ for single-photon emission. In the *left frame* the invariant mass of the $\mu^+\mu^-$ pair; SDP$= 0.00534$. In the *right frame* the invariant mass of $\mu^-\gamma$; SDP$= 0.00296$. The histograms produced by the two programs (logarithmic scale) and their ratio (linear scale, *black line*) are plotted in both frames. The fraction of events with hard photons was $17.4863 \pm 0.0042\%$ for KORALZ and $17.6378 \pm 0.0042\%$ for PHOTOS

two distributions generated by the compared programs superimposed on a single plot, often with a logarithmic scale. Such a method was used, for example, in [23]. The method is unquestionably sufficient, if one's interest is limited to, say, the collinear content of the results or other distributions of the intrinsically leading logarithmic type. In fact, in all our plots the lines obtained from PHOTOS and reference Monte Carlos cannot be separated by the eye. The inclusion of the *third* line representing the ratio of the two predictions was thus essential.

5 Results of the tests performed at first order

Let us start with a comparison of PHOTOS and KORALZ [25], both run at first order and without exponentiation.[8] The results from KORALZ are given by a red (darker gray) line and from PHOTOS by a green (lighter gray) line. (In the presentation of the results we use the colour coding consistently in the plots, following the methodology of MC-TESTER). The lines overlap almost completely on all plots, and only the ratios of the histograms (shown as black distributions) indicate that there is indeed some difference. In all comparisons presented in this section the samples of 10^8 events were used and *test1*, as defined in Sect. 3, was employed.

As it can be seen in Fig. 1, PHOTOS predicts a fraction of events about 0.15% larger with a photon (of energy above 1 GeV) than KORALZ. This difference, noticeable thanks to our method, is not large. The differences in the distributions reach about 15% in the areas of the phase space containing photons of extremely large energies and away from the direction of the muons. This difference may potentially be of importance for experimental physicist interested in backgrounds for some signatures of new physics.

Even though the agreement is amazing, it is yet improved once the NLO term is included into the correction weight of PHOTOS: the differences disappear below the statistical error of 10^8 event samples and all over the phase space! In the caption and plots of Fig. 2, we collect the results using exactly the same method as previously discussed, but for the runs with the NLO correcting weight activated in PHOTOS.

The agreement for the branching fractions (of events with and without photons of energy larger than 1 GeV) is better than 0.01% now! This indeed confirms that the effects that were missing previously are not only small, but of theoretical origin.[9]

6 Numerical results of the tests performed with multiple-photon radiation

Let us now turn to the tests of PHOTOS running in a multiple-photon option. For that purpose we use again *test1* as defined in Sect. 3, and samples of 10^8 events generated by the KKMC generator with second-order matrix element and exponentiation, and the multiple-photon ra-

[8] These results have been published (even though in different form) in [13], yet they are repeated here to serve as a reference for comparisons. This is true also in the case of Figs. 3 and 5.

[9] This is important, as it provides a powerful technical test of the generator. The kinematical variables used in PHOTOS differ from those of KORALZ; four-vectors are used instead of angles to parametrize the intermediate steps of the generation. The differences could have indicated, say, consequences of aggregation of rounding errors. Keeping in mind that similar levels of agreement for muons were achieved for the multi-photon version of PHOTOS and KKMC in the $Z \to e^+e^-$ decay channel, we can confidently claim that PHOTOS has its numerical stability under control. This was not the case for the early versions of the program, and reaching that level of technical reliability required a major effort.

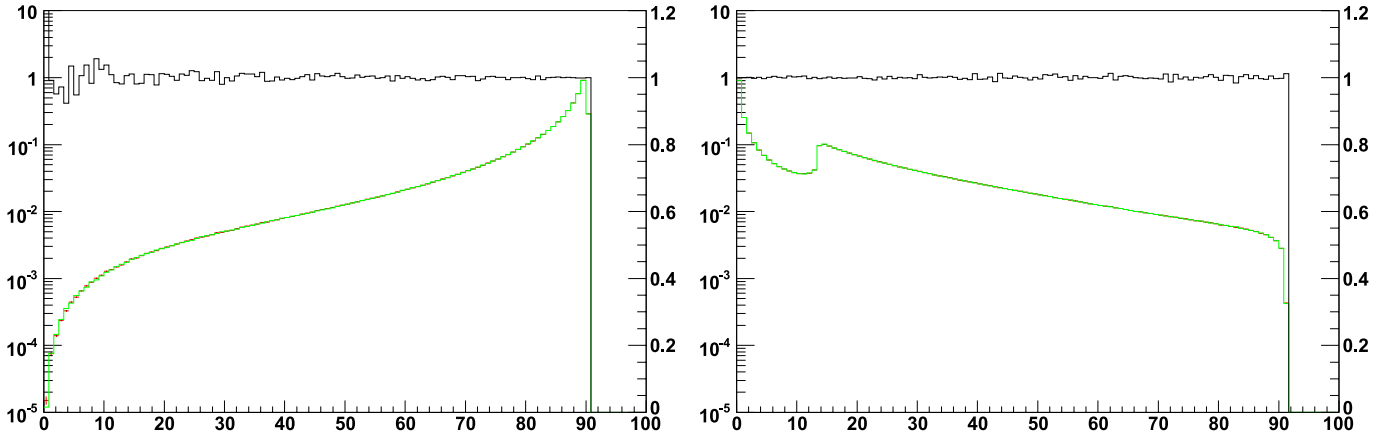

Fig. 2. Comparisons of improved PHOTOS and KORALZ for single-photon emission. In the *left frame* the invariant mass of the $\mu^+\mu^-$ pair. In the *right frame* the invariant mass of $\mu^-\gamma$ pair is shown. In both cases differences between PHOTOS and KORALZ are below statistical error. The fraction of events with hard photons was $17.4890 \pm 0.0042\%$ for KORALZ and $17.4926 \pm 0.0042\%$ for PHOTOS

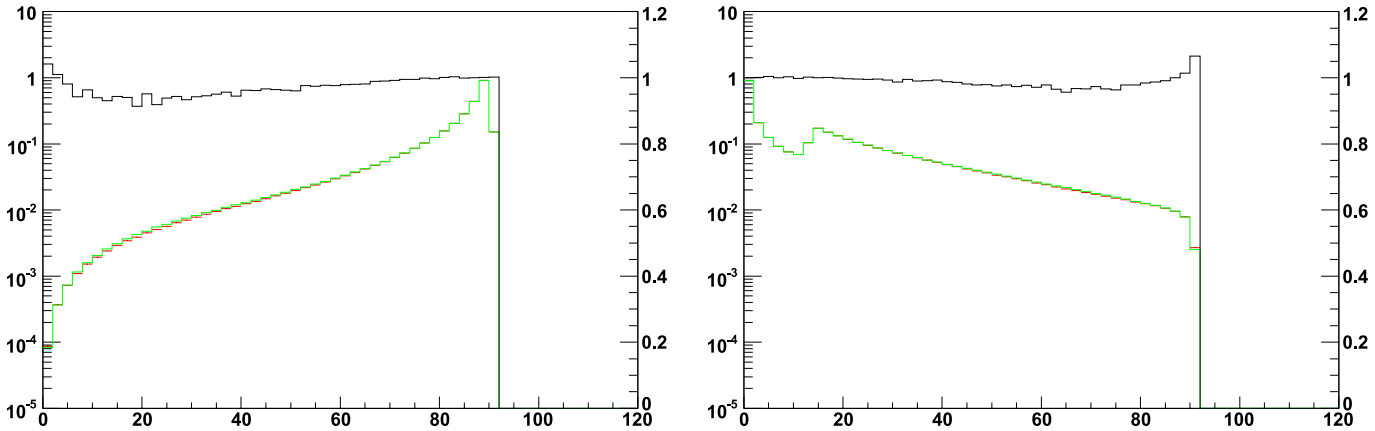

Fig. 3. Comparison of standard PHOTOS with multiple-photon emission and KKMC with second-order matrix element and exponentiation. In the *left frame* the invariant mass of the $\mu^+\mu^-$ pair; SDP$= 0.00409$. In *right frame* the invariant mass of the $\mu^-\gamma$ pair; SDP$= 0.0025$. The pattern of differences between PHOTOS and KKMC is similar to the one of Fig. 1. The fraction of events with hard photons was $16.0824 \pm 0.0040\%$ for KORALZ and $16.1628 \pm 0.0040\%$ for PHOTOS

diation version of PHOTOS, without NLO terms. The results are presented in Fig. 3.

The pattern of differences for the multi-photon runs of PHOTOS and KKMC is similar to the one at the first order (Fig. 1). The black line showing the KKMC-to-PHOTOS histograms' ratios indicates the differences mostly for the configurations with hard photons; that is, for the regions of phase space where histograms are sparsely populated. The differences reach a few per cent in the corners of the phase space contributing a few per mille to the total rate. The discrepancies are below 0.1% with respect to the total rate.

Once the NLO weight in PHOTOS is activated, see Fig. 4, the differences become even smaller, by a factor of order of 50 (again, samples of 10^8 events were used). This confirms that the main source of residual discrepancy between KKMC and standard PHOTOS, as seen in Fig. 3, was due to the NLO terms missing there. This conclusion seem to be contradicted by the "naked-eye" inspection of Figs. 3 and 4, where the ratios look quite similar. There is not much improvement at the very end of the distributions for the bins by more than 2 orders less populated than dominant ones. On the other hand, for more populous bins, the differences diminished.

Let us now turn to *test2*, where configurations of up to two hard photons are analyzed. We will firstly present the results of a comparison of the standard multiple-radiation version of PHOTOS with that of KKMC (with second-order matrix element and exponentiation), followed by the comparison of multiple-radiation version PHOTOS with NLO weight and again with KKMC. Again, we drop most of the plots and present only those, for two hard-photon configurations, where SDP was largest, for the cases where the NLO kernel was active in PHOTOS and the ones where it was not. These are respectively invariant mass of $\mu^+\mu^-$ and of $\gamma\gamma$ pairs.

One can see from Fig. 5, that already for the standard PHOTOS the agreement with KKMC is good. Residual deficiencies are rather small also for the two hard-photon configurations. From Fig. 6, one can conclude that the inclusion of NLO terms in PHOTOS improves the agreement

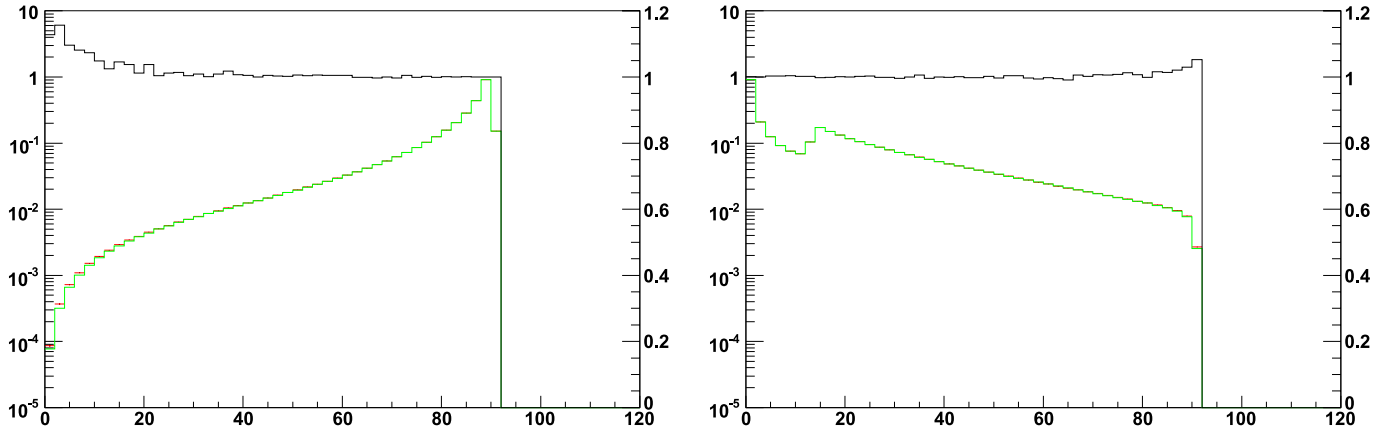

Fig. 4. Comparisons of improved PHOTOS with multiple-photon emission and KKMC with second-order matrix element and exponentiation. In the *left frame* the invariant mass of the $\mu^+\mu^-$ pair; SDP$= 0.0000249$. In the *right frame* the invariant mass of the $\mu^-\gamma$ pair; SDP$= 0.0000203$. The fraction of events with hard photons was $16.0824 \pm 0.004\%$ for KORALZ and $16.0688 \pm 0.004\%$ for PHOTOS

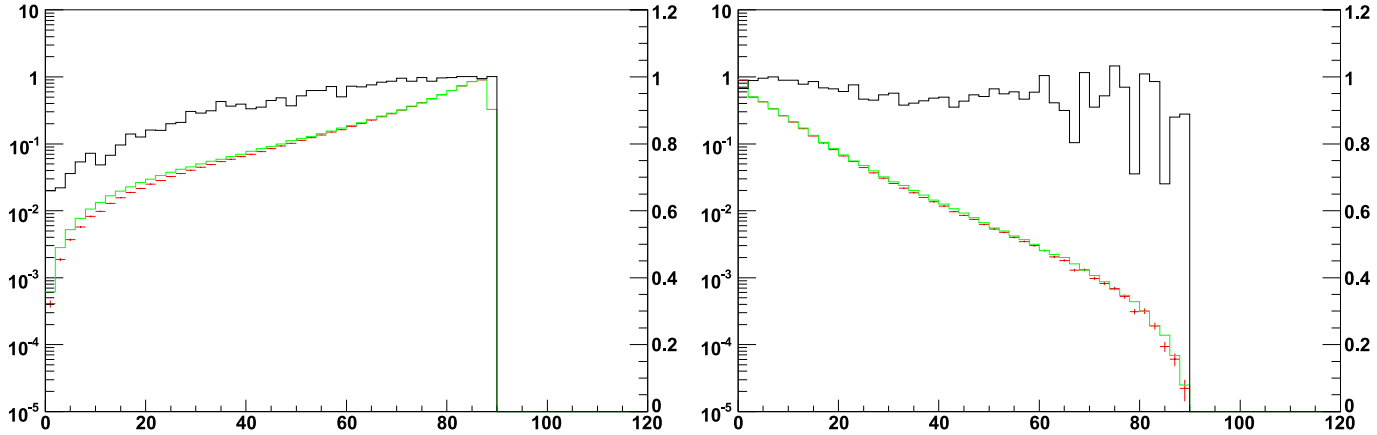

Fig. 5. Comparisons of standard PHOTOS with multiple-photon emission and KKMC with second-order matrix element and exponentiation. In the *left frame* the invariant mass of the $\mu^+\mu^-$ pair; SDP$= 0.00918$. In the *right frame* the invariant mass of the $\gamma\gamma$ pair; SDP$= 0.00268$. The fraction of events with two hard photons was $1.2659 \pm 0.0011\%$ for KORALZ and $1.2952 \pm 0.0011\%$ for PHOTOS

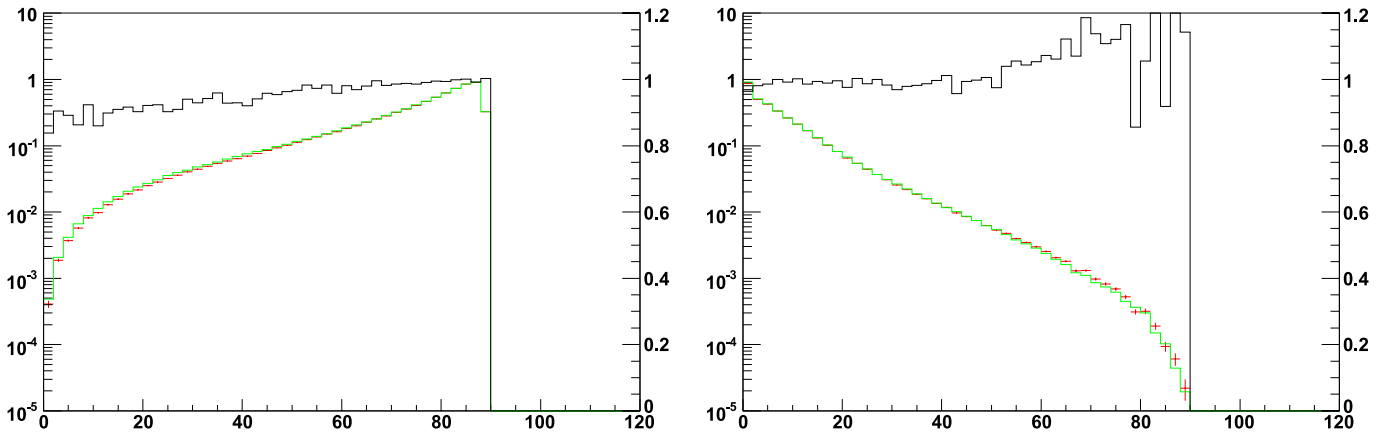

Fig. 6. Comparisons of improved PHOTOS with multiple-photon emission and KKMC with second-order matrix element and exponentiation. In the *left frame* the invariant mass of the $\mu^+\mu^-$ pair; SDP$= 0.00142$. In the *right frame* the invariant mass of the $\gamma\gamma$; SDP$= 0.00293$. The fraction of events with two hard photons was $1.2659 \pm 0.0011\%$ for KORALZ and $1.2868 \pm 0.0011\%$ for PHOTOS

with KKMC even further. Quantified in *test2* with SDP, it improves by about a factor of 6. This is encouraging, as for some of the distributions, to improve, the inclusion of the second-order matrix element seems to be imperative.

We also observed that for standard PHOTOS the differences in the ratios are relatively large in the end part of the $\mu^+\mu^-$ pair mass. The differences consecutively grow for an invariant mass below 30 GeV, from a few percent up to about 35% at the lowest masses. The shape of this difference is similar to the one in the spectrum of $\mu^+\mu^-$ mass in the single-photon case (Fig. 1). Now the differences seem to be larger by about a factor of 2. This somewhat naive observation gets confirmed if NLO terms are switched on. The difference between PHOTOS and KKMC improved by about factor of 6 with respect to Fig. 5 where standard PHOTOS was used. These differences, as can be seen in Fig. 6, approach only 10% in the end part of the $\mu^+\mu^-$ invariant mass spectrum. For the $\gamma\gamma$ invariant mass above $M_Z - 10\,\mathrm{GeV}$, the differences approach about 15%. The case of improved PHOTOS results remains similar to the unimproved one. Quantified with SDP it actually increased by about 10%.

The maximum of SDP calculated for all plots of *test2* decreased by a factor of about 3, and only for the case of $\gamma\gamma$ invariant mass it increased by 10%. For all other comparison plots (skipped in the paper but available in [29]) the individual SDP's were smaller and decreased. The improvement is numerically not as striking as for the single hard-photon configurations; this should be no surprise: the complete second-order matrix element is missing, and it is necessary to obtain even lowest order *test2* observables involving simultaneously two hard photons. The improvement by a factor of 3 provides, however, a strong indication that the algorithm of iteration used in the generation of consecutive photons works well from the perspective of NNLO as well. The acoplanarity plots presented in [13] demonstrate the NNLO performance of our algorithm as well. We are not going to discuss this point here, but we would rather leave it to a future discussion of the NNLO content of our algorithm: this aspect goes beyond the purpose of the present paper and the interest of most of PHOTOS users.

As much as for the NLO effects discussed in the present paper, a new contribution to the PHOTOS correcting weight would be needed for the NNLO. However no changes in the phase-space algorithm would a priori be required. The techniques of gauge-invariant separation of the amplitudes into parts, as used for instance in [26], will probably be necessary. They proved to be instrumental in the implementation of the second-order matrix elements for $e^+e^- \to \nu_e\bar{\nu}_e\gamma\gamma$ into KKMC. The exclusive exponentiation scheme of the KKMC Monte Carlo is prepared for s-channel processes.

We have to admit that once the NLO terms were switched on in PHOTOS, the difference with KKMC were at the limit of being recognizable, even if samples of 10^8 events are used. For the case of the two-photon test, differences due to the missing second-order matrix element in PHOTOS can be observed; yet they are too small, and do not have enough structure to explore their possible origin. A part of the differences may even originate from the third-order LL terms (after integration), which are missing in KKMC but are generated in PHOTOS in the process of iteration. This makes a conclusion on the nature of NNLO effects missing in PHOTOS rather impossible.

In any case, even for PHOTOS running with standard options, the differences affect only a tiny fraction of the Z decay phase space. Thus, we do not consider it to be of much practical interest to continue the discussion or to implement the missing terms. This could have been a particularly interesting aspect of the study for the attempts to extend our algorithm to QCD.

7 Summary

To quantify the size of the NLO effects, which are normally missing in PHOTOS we reinstalled them into the program, using the complete first-order expression for leptonic Z decay. After the NLO correcting weight was installed, the differences between PHOTOS and KORALZ (both run at first-order without exponentiation) were below the statistical error of 10^8 events for all the distributions used in the tests. The agreement provides an important technical test for the two simulations. For the case of multiple-photon radiation in PHOTOS, a comparison with the KKMC generator [14] (exponentiation and second-order matrix element used) was performed. The implementation of the NLO terms in PHOTOS indicated an improvement by a factor of about 50 for the observables sensitive to a single hard photon in the final states and remained at the level of better than 0.1% on the total rate for all other cases we examined. Because of the smallness of the residual differences, it was difficult to understand their structure and origin in the final states with two hard photons.

The improvement due to the introduction of the NLO correcting weight came at a price. Even though the weight is analytically simple and the generation of weight 1 events remained possible, the calculation of the weight required information on the Born-level coupling constants of the intermediate Z/γ^*. Also, the direction of the beam was necessary in the calculation of the weight. These requirements are contrary to the modular organization of the PHOTOS solution, as used in the large Monte Carlo generation chains of experimental collaborations. Numerically, the improvements are rather small and the imperfections of standard PHOTOS are localized in the corners of bremsstrahlung phase space populated by photons of very high energies and angularly well separated from the final-state muons. Those regions of the phase space weigh less than 0.005 to the total rate, and the differences in that region approach 20% of their size. The effects are thus less than 0.1% of the total rate of the Z decay to muons. That is why we do not think it justified to complicate the PHOTOS algorithm and to enable the use of the NLO correcting weight in the general case.

The analysis presented here concentrates not only on the numerical results for the final-state bremsstrahlung in

Z decay, but also on various aspects of the mathematical organization of the program for the calculation of radiative corrections in Z production and decay. Separation of radiative corrections into parts were mentioned as well: (i) ones embodied in effective couplings of the hard-scattering process, (ii) final-state QED bremsstrahlung, and (iii) initial-state bremsstrahlung, eventually with initial-state hadronic interactions. The effects of QED initial–final-state bremsstrahlung interference were to a large degree neglected. Such an approach is reasonable in the leading-pole approximation for the Z, but at a certain precision level the effects may need to be taken care of. For the time being the results of [27] can be used instead.

Thanks to the analytic form of the kernel used in PHOTOS for the single-photon emission, the analysis presented here may easily be extended to other decay channels, if a high precision is required and a calculation of matrix elements is available. The study for the case of B meson decay into a $\pi^{\pm}(K^{\pm})$ pair, where non-relativistic details of phase-space parametrization are given, is now completed [28]. In this case the question of the reliability of scalar QED for the calculation of photons of high p_{T}, with respect to charged scalars, needs to be addressed. A natural extension of the study of the systematic error in PHOTOS simulations, as presented here, would be the discussion of bremsstrahlung in W and Higgs boson decays.

The decays of the W and Higgs bosons are probably the only ones where formal studies of the NLO terms, similar to the ones presented in this paper, can be performed. As was the case with Z decays, those cases will also be limited to the leading-pole approximation.

For other decay channels, the correction weight can be applied as well; however, in most cases the part of the weight going beyond soft and/or collinear regimes may need to be constructed with the help of the fits to the data. Let us stress that the unique design of PHOTOS, enabling the use of the same kernel for multiple-photon radiation (exponentiated) mode and at fixed first, second, third, and fourth orders, establishes a convenient environment for such fits of the form factors to the data. At the same time the analytical form of such form factors can be taken from the first-order analytic calculations based on effective theory, or from any other model. Technically the NLO correcting weight of PHOTOS is integrated as an internal correcting weight.[10]

Finally, let us stress that the approximations introduced in PHOTOS affect only the matrix elements and not the phase space. The generation of the latter is based on the tangent space constructed from an eikonal approximation and used also for hard photons, even of energies above the available maximum enforced by energy-momentum conservation. This is similar to the case of the classical exclusive exponentiation. However, the energy-momentum constraints are introduced for each individual photon step by step. Conformal symmetry is not used in that procedure.

In principle, if necessary, complete higher-order matrix elements can be incorporated with the help of correcting weights. This point goes beyond the scope of the present paper. This is equally true for the possible extensions of PHOTOS algorithm to simulations in QCD.

Acknowledgements. Useful discussions with Dmitri Bardin, Borut Kersevan, Maarten Bonekamp and Daniel Froidevaux are acknowledged. Special thanks go to Torbjörn Sjöstrand whose critical remarks convinced us of the necessity and urgency to perform the presented work.

[10] This is important, because it points to the possibility of repeating the study presented here for any other distribution. That is, for realistic observables as those used in future or past measurements.

References

1. E. Barberio, B. van Eijk, Z. Was, Comput. Phys. Commun. **66**, 115 (1991)
2. E. Barberio, Z. Was, Comput. Phys. Commun. **79**, 291 (1994)
3. M.A. Dobbs et al., http://www.arXiv.org/abs/hep-ph/0403045
4. CDF Collaboration, V.M. Abazov et al., Phys. Rev. D **70**, 092 008 (2004), http://www.arXiv.org/abs/hep-ex/0311039
5. OPAL Collaboration, G. Abbiendi et al., Phys. Lett. B **580**, 17 (2004), http://www.arXiv.org/abs/hep-ex/0309013
6. DELPHI Collaboration, J. Abdallah et al., Eur. Phys. J. C **31**, 139 (2003), http://www.arXiv.org/abs/hep-ex/0311004
7. NA48 Collaboration, A. Lai et al., Phys. Lett. B **602**, 41 (2004), http://www.arXiv.org/abs/hep-ex/0410059
8. KTeV Collaboration, T. Alexopoulos et al., Phys. Rev. D **71**, 012 001 (2005), http://www.arXiv.org/abs/hep-ex/0410070
9. Belle Collaboration, A. Limosani et al., http://www.arXiv.org/abs/hep-ex/0504046
10. BABAR Collaboration, B. Aubert et al., Phys. Rev. D **69**, 111 103 (2004), http://www.arXiv.org/abs/hep-ex/0403031
11. FOCUS Collaboration, J.M. Link et al., http://www.arXiv.org/abs/hep-ex/0412034
12. P. Golonka, Z. Was, http://www.arXiv.org/abs/hep-ph/0508015
13. P. Golonka, Z. Was, Eur. Phys. J. C **45**, 97 (2006), http://www.arXiv.org/abs/hep-ph/0506026
14. S. Jadach, Z. Wąs, B.F.L. Ward, Comput. Phys. Commun. **130**, 260 (2000); up to date source available from http://home.cern.ch/jadach/
15. S. Jadach, B.F.L. Ward, Z. Was, Phys. Rev. D **63**, 113 009 (2001), http://www.arXiv.org/abs/hep-ph/0006359
16. A. Nikiforov, Y. Ouvarov, Éléments de la Théorie des Fonctions spéciales (Editions Mir, Moscow, 1976)
17. F.V. Tkachov, Sov. J. Part. Nucl. **25**, 649 (1994), http://www.arXiv.org/abs/hep-ph/9701272
18. Z. Was, Written on the basis of lectures given at the 1993 European School of High Energy Physics, Zakopane, Poland, 12–25 September 1993, http://www.arXiv.org/abs/CERN-TH-7154-94

19. S. Jadach, Z. Was, R. Decker, J.H. Kühn, Comput. Phys. Commun. **76**, 361 (1993)
20. F. James, FOWL – a General Monte Carlo Phase Space Program, 1977, CERN Computer Centre Program Library, Long Writeup W505
21. F.A. Berends, R. Kleiss, S. Jadach, Nucl. Phys. B **202**, 63 (1982)
22. R. Kleiss, Nucl. Phys. B **347**, 67 (1990)
23. K. Hamilton, P. Richardson, http://www.arXiv.org/abs/hep-ph/0603034
24. P. Golonka, T. Pierzchała, Z. Was, Comput. Phys. Commun. **157**, 39 (2004), http://www.arXiv.org/abs/hep-ph/0210252
25. S. Jadach, B.F.L. Ward, Z. Was, Comput. Phys. Commun. **66**, 276 (1991)
26. Z. Was, http://www.arXiv.org/abs/hep-ph/0406045
27. S. Jadach, Z. Was, Phys. Lett. B **219**, 103 (1989)
28. G. Nanava, Z. Was, http://www.arXiv.org/abs/hep-ph/0607019
29. http://cern.ch/Piotr.Golonka/MC/PHOTOS-MCTESTER/AtNLO